Strange hadron effective temperatures in relativistic nuclear collisions

Oana Ristea[1], Catalin Ristea[1,2], Alexandru Jipa[1], Ionel Lazanu[1], Marius Calin[1], Tiberiu Esanu[1,3]

[1]University of Bucharest, Faculty of Physics, [2]Institute of Space Science,

[3]National Institute of Nuclear Physics and Engineering Horia Hulubei, Bucharest-Magurele, Romania

Introduction

QGP production in relativistic heavy-ion collisions may be signaled by the non-monotonous energy dependence of several hadronic observables such as the strangeness and pion yields in the phase transition region.

In Ref.1, it was suggested that a signal of the phase transition from hadron gas to QGP could be a plateau-like behavior in the dependence of the average transverse momentum on the hadron multiplicity. The $\langle p_T \rangle$ can be correlated with the temperature and collective flow of the system, whereas the produced hadron multiplicity is a measure of the entropy produced in a high energy collision. The saturation of $\langle p_T \rangle$ during the mixed phase could indicate a rapid increase in the number of degrees of freedom, followed by a second rise when the matter undergoes a structural change to its colored constituents.

The constant effective temperature of $K^{\pm}$ in the SPS energy range was interpreted as a consequence of the coexistence of hadronic and deconfined phases.

Results – charged kaons

The effective temperatures were extracted from the transverse momentum spectra using the exponential function:

$$\frac{1}{2\pi p_T}\frac{d^2N}{dp_T\,dy} = \frac{dN/dy}{2\pi T(T+m)}\cdot\exp\left(-\frac{m_T-m}{T}\right)$$

where m is the particle rest mass, m_T is the transverse mass, dN/dy is the yield and T is the inverse slope or the effective temperature. However, T does reflect not only the temperature of the system at the kinetic freeze-out because is sensitive to both the thermal and transverse collective motion.

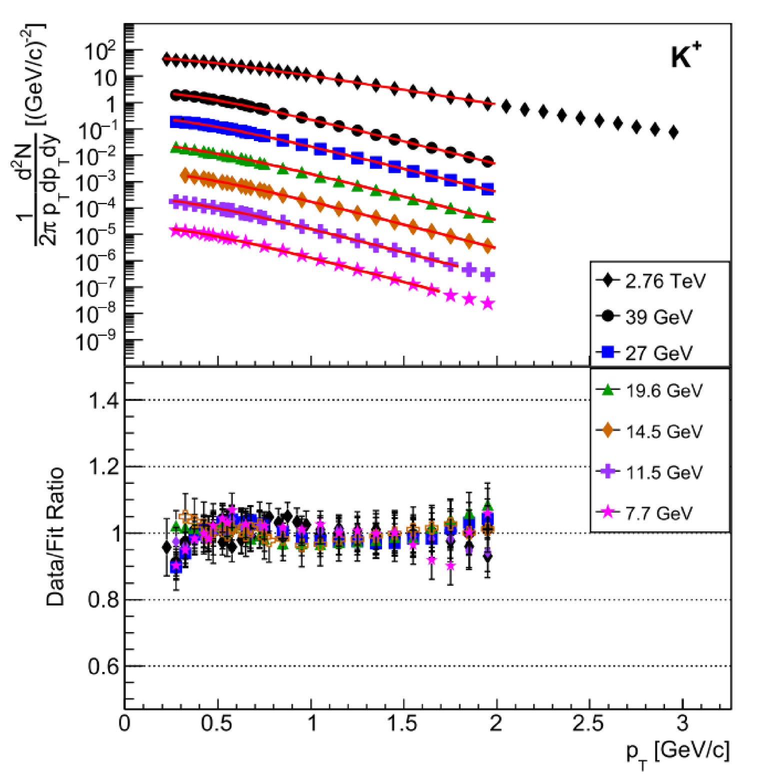

Fig. 1. Top: Transverse momentum spectra of positive kaons produced in most central Pb + Pb collisions (0–5% centrality) at $\sqrt{s_{NN}}$ = 2.76 TeV and Au + Au collisions (0–5% centrality) at $\sqrt{s_{NN}}$ = 39, 27, 19.6, 14.5, 11.5 and 7.7 GeV. Red lines are the exponential fits to data using Eq. (1). Bottom: Data/Fit ratios as a function of transverse momentum.

Results – charged kaons

T(K^+) and T(K^-) as a function of energy from most central Au+Au collisions at RHIC-BES energies, Au+Au collisions at AGS energies, Pb+Pb collisions at SPS energies, Au+Au collisions at RHIC energies and Pb+Pb collisions at $\sqrt{s_{NN}}$ = 2.76 TeV are shown in Fig.2.

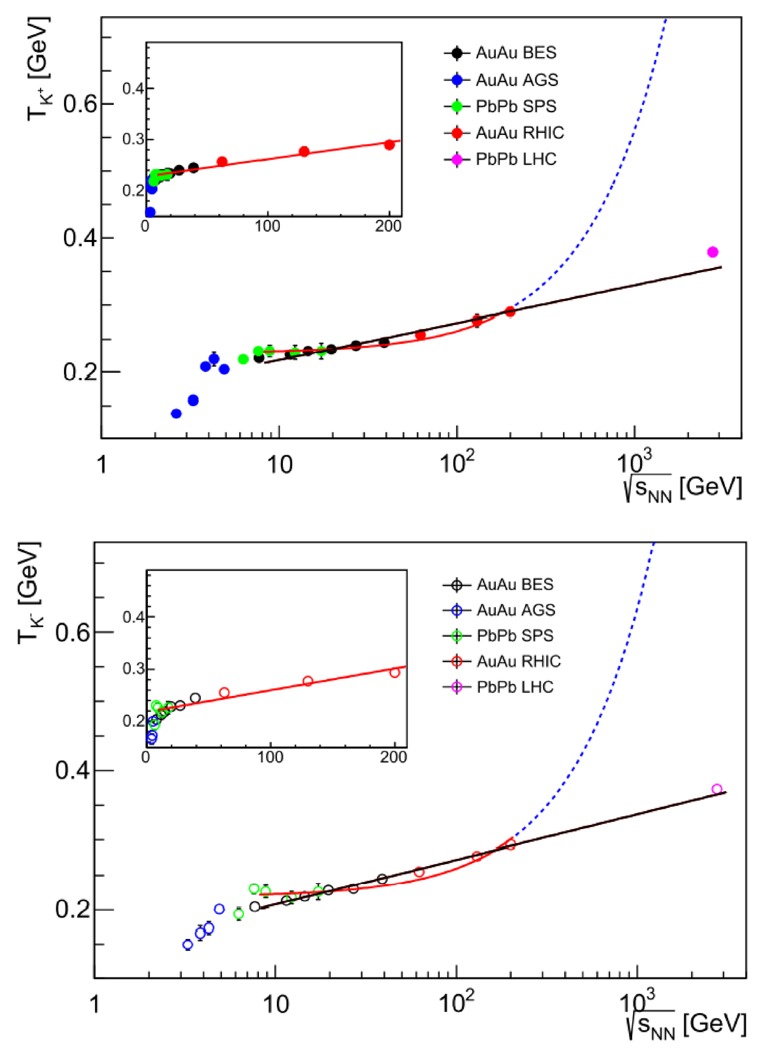

The energy dependence of the data shows a sudden change around $\sqrt{s_{NN}}$ = 7–8 GeV. Above this energy T is showing a slower increase than at lower energies. Such a trend with energy was analyzed using a linear and a logarithmic dependence.

The solid lines represent the linear (red) and logarithmic (black) fits. The linear fit is extrapolated from RHIC highest energy up to LHC energy (blue dotted curve).

Because the pions are the most abundantly produced particles in the relativistic nuclear collisions, the pion rapidity density is used as a measure of the produced entropy.

$$dN/dy_\pi = 1.5\cdot(dN/dy_{\pi^+}+dN/dy_{\pi^-})$$

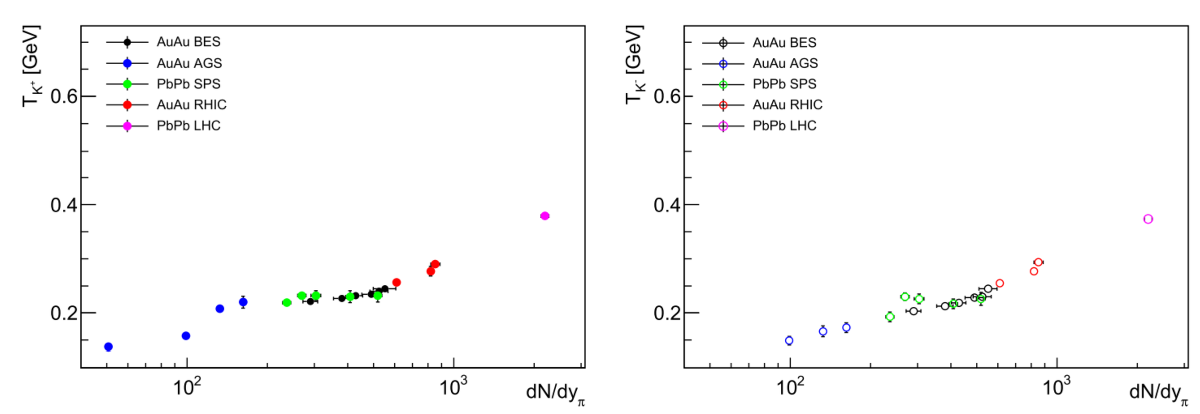

Fig. 3: T(K+) and T(K-) as a function of pion dN/dy in most central Au + Au collisions at RHIC-BES energies (black symbols). Also shown are the results from AGS, SPS and LHC.

T(K^+) increases with dN/dy_π at AGS energies. At higher energies, above $\sqrt{s_{NN}}$ = 8 GeV, there is a slower, continuous rise with energy up to LHC energy. Such behavior may reflect the characteristic signature of a first-order phase transition and could have the origin in the modification of the equation of state of the matter due to the deconfined phase transition.

T(K^-) increases slowly over the entire energy range from AGS to LHC energies.

Results – Ω^-

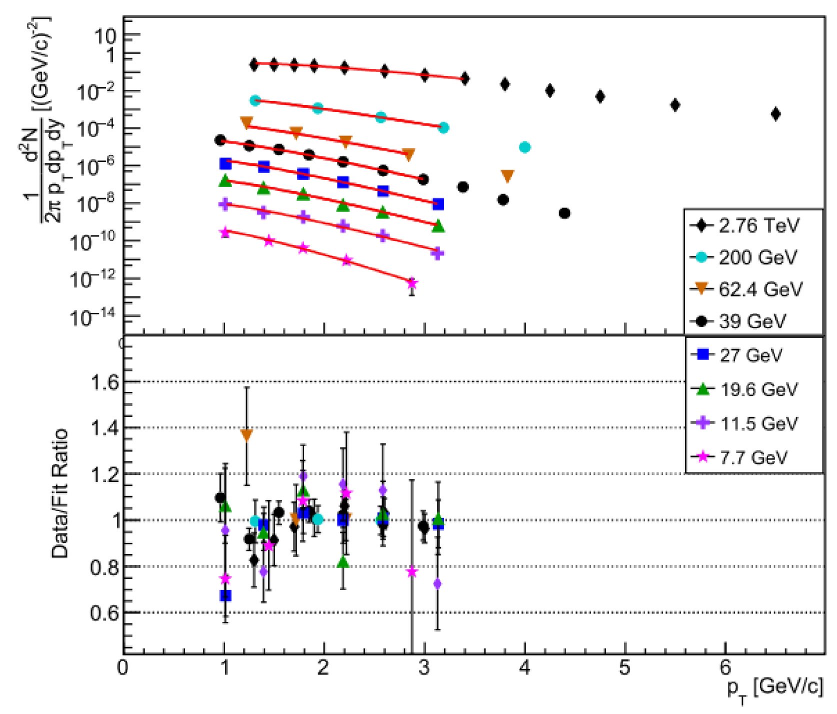

Fig.4: Ω^- p_T spectrum in Pb + Pb collisions at $\sqrt{s_{NN}}$ =2.76 TeV, $\Omega^- + \Omega^+$ p_T spectrum in Au+Au collisions at $\sqrt{s_{NN}}$ = 200 GeV and Ω^- p_T spectra obtained in Au+Au collisions at $\sqrt{s_{NN}}$ = 62.4, 39, 27, 19.6, 11.5 and 7.7 GeV.

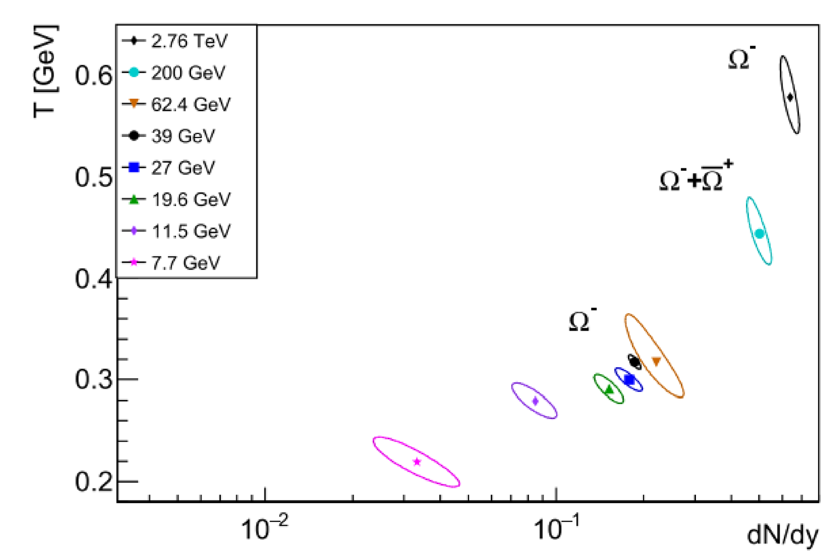

Fig.5: Contour plot of Ω^- and Ω^+ effective temperatures and rapidity densities. The best fit values are shown with points, lines are 1σ contours.

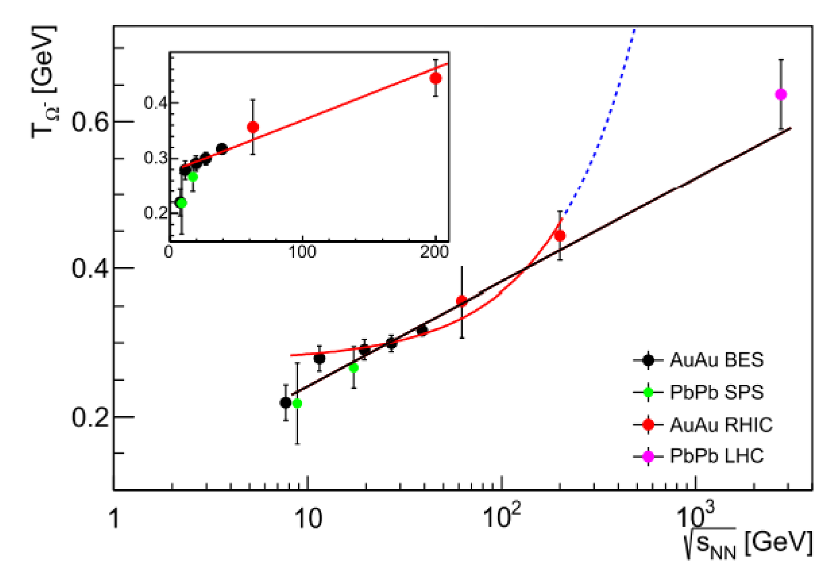

Fig.6: Energy dependence of the Ω^- effective temperatures. The solid lines represent the linear (red) and logarithmic (black) fits. The linear fit is extrapolated from RHIC at higher energies (blue dotted curve). Insert figure: The same data and the linear fit for 0–200 GeV energy range.

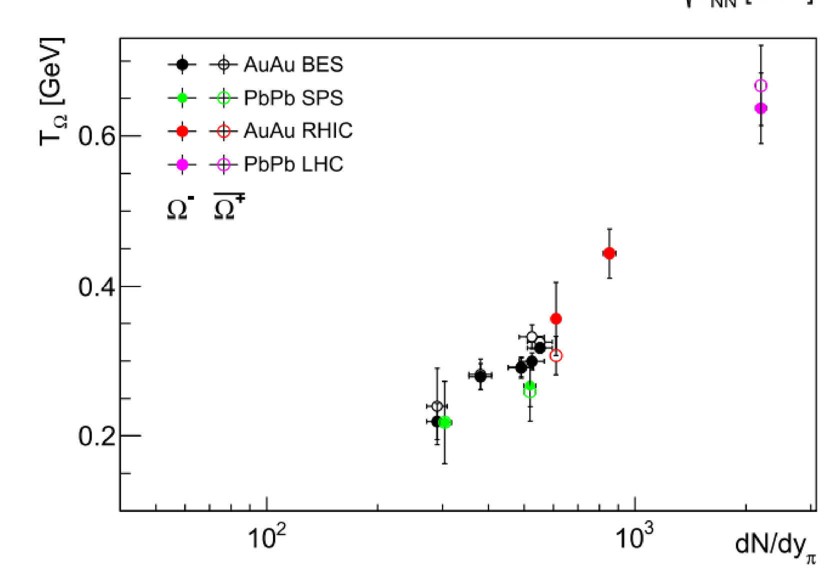

Fig.7: T(Ω^-)as a function of the pion rapidity densities, dN/dy, in relativistic heavy-ion collisions.

The SPS and BES results are consistent within errors.

The energy dependence of T for Ω^- and φ is better described by the logarithmic function over the entire energy range studied.

Results - φ

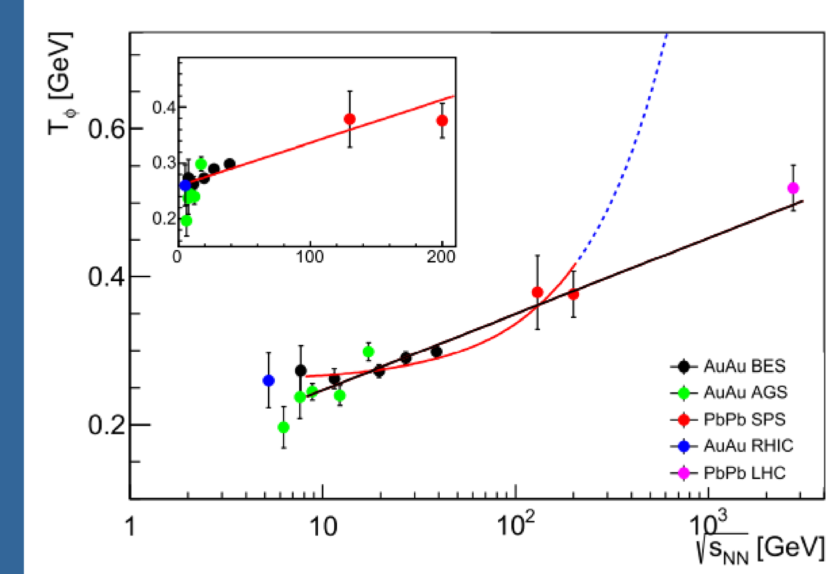

Fig.8: Slope parameter Tφ as a function of energy. The solid lines represent the linear (red) and logarithmic (black) fits. The linear fit is extrapolated from $\sqrt{s_{NN}}$ = 200 GeV to higher energies (blue dotted curve). Insert figure: The same data and the linear fit for the 0–200 GeV energy range.

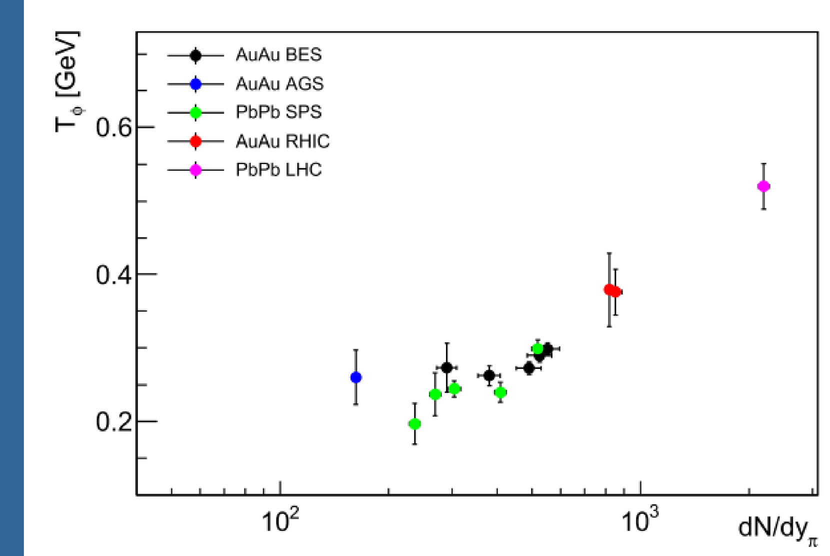

Fig.9:φ effective temperatures as a function of the pion rapidity densities, dN/dy, in Au + Au collisions at RHIC-BES energies (black symbols). Also shown are results from experiments at the AGS, SPS, RHIC and LHC.

Conclusions

The energy dependence of the $K^{\pm}$ and φ effective temperatures exhibits different trends before and after $\sqrt{s_{NN}}$ = 7–8 GeV. Above $\sqrt{s_{NN}}$ ~ 8 GeV, slope parameters are showing slower increase than at lower energies. This behavior is similar within errors to what was observed at SPS energies and could indicate the onset of the deconfinement at these energies.

For the Ω^- inverse slope parameters, a similar behavior is observed at energies larger than $\sqrt{s_{NN}}$ ~ 8 GeV. However, the sudden change in the energy dependence below this energy is not visible, as no data are available in this energy range.

References

L. Van Hove, Phys. Lett. B 118 (1982) 138; STAR Collab. (L. Adamczyk et al.), Phys. Rev. C. 96 (2017) 44904; STAR Collab. (J. Adam et al.), arXiv:1908.03585 [nucl-ex]; ALICE Collabs. (B. Abelev et al.), Phys. Rev. C 88 (2013) 044910; E866 and E917 Collab. (L. Ahle et al.), Phys. Lett. B 490 (2000) 53; E866 and E917 Collab. (L. Ahle et al.), Phys. Lett. B 476 (2000) 1; NA49 Collab. (C. Alt et al.), Phys. Rev. C. 77 (2008) 024903; NA49 Collab. (S. V. Afanasiev et al.), Phys. Rev. C. 66 (2002) 054902; BRAHMS Collab. (I. Arsene et al.), Phys. Lett. B 687 (2010) 36; STAR Collab. (C. Adler et al.), Phys. Lett. B. 595 (2004) 143; PHENIX Collab. (S. S. Adler et al.), Phys. Rev. C. 69 (2004) 034909.

Acknowledgements

This work was supported by ANCS through 5/5.2/FAIR-RO Program - FAIR08/2020 contract with IFA.